buildings

MDPI

Article

Effect of Natural Pozzolan and Waste Glass Powder on the Mechanical Properties of Mortars Containing Polypropylene Fibers Utilizing Response Surface Methodology

Muhammad Iftikhar Khan, Mohammed K. Alkharisi *, Hany A. Dahish and Muhammad Ibrahim

Department of Civil Engineering, College of Engineering, Qassim University, Buraidah 52571, Saudi Arabia; 451116622@qu.edu.sa (M.I.K.); ha.dahish@qu.edu.sa (H.A.D.); 472118105@qu.edu.sa (M.I.)

* Correspondence: m.alkharisi@qu.edu.sa

Abstract

This research shows the combined effects of natural pozzolan (NP) and waste glass powder (WGP) on the mechanical strength of polypropylene fiber (PPF)-reinforced cement mortars. As the construction sector is looking for alternatives to traditional binding materials, this study addresses the challenge of reducing carbon footprints. A dataset of 405 test results for compressive strength (fc), tensile strength (ft) and flexural strength (fr) was used to model and optimize the impact of partial replacement of cement with NP and WGP at replacement levels up to 20 and 30% by weight, respectively, and PPF at volume levels of 0.5 and 1.5% on the strengths of mortars utilizing response surface methodology (RSM). A solution combining sodium hydroxide and sodium silicate (SH + SS) is utilized at a constant ratio. The results show that all mixes gained strength with curing age, increasing WGP generally reduced the strength at all ages, and a moderate NP content (10%) gave the highest compressive and tensile strengths. The importance and applicability of established models were evaluated, and the contributions of the variables were examined using analysis of variance (ANOVA) along with other statistical tests. Numerical optimization was utilized to identify the optimal NP, WGP, and PPF values for optimizing mortar mechanical properties. The statistical models generated via RSM exhibited high coefficients of determination (R^2) of 0.9835, 0.9775, and 0.921 for fc, ft, and fr, respectively, indicating the reliability of the design in predicting mortar behavior. The highest measured strengths were obtained with 0.5% PPF, while the multi-response optimization gave about 1.0% PPF when the cement replacement was also maximized. The study concludes that an optimized blend of NP and WGP can produce eco-friendly mortars that meet structural requirements for specific masonry applications.

Keywords: natural pozzolan; waste glass powder; polypropylene fibers; mechanical properties; response surface methodology; optimization

Check for updates

Academic Editor: Ahmet Benli

Received: 4 September 2026
Revised: 28 September 2026
Accepted: 5 October 2026
Published: 16 October 2026

Copyright: © 2026 by the authors. Licensee MDPI, Basel, Switzerland. This article is an open access article distributed under the terms and conditions of the Creative Commons Attribution (CC BY) license.

1. Introduction

Concrete's remarkable durability and ability to support compressive stresses make it an adaptable building material. Cement, serving as the primary binding agent in concrete, generates substantial carbon dioxide emissions throughout its manufacturing, contributing significantly to energy consumption and environmental degradation. The manufacturing of cement was responsible for 2.4 gigatons of CO_2 emissions in 2019, or 26% of all industrial emissions (IEA, 2020), which is alarming [1]. Emissions in 2015 were 30% less than those

later recorded by the Global Carbon Project [2], and in 2016 they were 1.45 ± 0.20 Gt, or around 4% of fossil fuel emissions. This suggests an annual rise.

To maintain sustainable growth, it is crucial to reduce emissions of CO_2 from global manufacturing of cement. To achieve this, a number of techniques have been developed, such as the introduction of innovative cement substitutes based on clinker, alkali-activated materials, and the improvement of cement efficiency. Reducing the cement used in concrete would help achieve both goals [3]. Supplemental cementitious materials (SCMs) are among the alternate materials that have been suggested as partial replacements for cement. Although they have reduced CO_2 emissions and cost of ingredients, their use as a replacement to cement in construction to improve attributes displays complicated behavior. Almotaseembillah, in his article published in 2024, reviewed various SCMs and their impact on different properties of concrete. He found that SCMs such as silica fume (SF), metakaolin (MK), and ground granulated blast furnace slag (GGBFS) improve compressive strength and resistance against chloride penetration, and increase the microstructural-level density at certain levels of addition [4]. Sherbaf et. Al., while undertaking a study of the impact of fly ash and natural pozzolan on self-consolidating concrete in 2022, found out that natural pozzolan performed equivalent to fly ash, exhibiting its great characteristics for use in concrete [5].

There are many studies on using natural pozzolan in conventional and alkali-activated concrete. In one such study, Khan and Alhozaimy (2011) looked at how NP affected the mechanical and physical characteristics of concrete [6]. After 28 days, they discovered that concrete mixes containing fifteen percent natural pozzolan showed a compressive strength that was comparable to plain concrete, using fifteen, twenty, and twenty-five percent of NP to replace cement content by weight. Furthermore, Najmi and Ghafoori (2018) discovered that substituting 13% of cement with NP led to a 2.2% boost in 56-day compressive strength and significant environmental benefits, such as a 12.34% reduction in energy and a 120 kg-CO_2-eq decrease per cubic meter of concrete [7]. Ramezanianpour et al. (2021) achieved remarkable results using a combination of 15% NP and 4% nano-silica to increase strength by 51.9% [7].

Other SCMs such as WGP have been thoroughly studied as a substitute for cement; when 20–30% of cement is substituted, a discernible improvement is seen. For instance, Li et al. (2022) studied the pozzolanic activity of WGP in mortar and discovered that, despite a 9.6% rise at 90 days, 20% replacement does not lower the strength on longer runs [8]. In a similar way, Jochem et al. (2020) discovered that replacing 10–20% of cement with WGP improves hydration kinetics and water retention [9]. These results imply that WGP can successfully lower the cement concentration without compromising the mortar's functionality, especially when the particle size is carefully regulated. Like NP, WGP helps produce C-S-H, which increases mortar's strength. Because both of these materials reduce reliance on OPC, they are perfect for sustainable green mortar, which lowers carbon emissions during construction. The combined synergistic effects of WGP and NP have not received much attention, which makes them an intriguing field for further study. The most frequent conclusion from most of the articles is that 20–30% of WGP should be used in place of cement to maintain strength and durability over time.

Waste glass powder (WGP) and natural pozzolan (NP) are pozzolanic materials with relatively low early age reactivity and, thus, their direct use as high-volume cement replacement materials is limited. Alkali activation speeds up geopolymeric reactions and improves the formation of strength and durability by facilitating dissolving of silica and alumina phases. According to research by Adewumi et al. (2020) and others, changing the SS/SH solution by 30%, 40%, and 50% by binder weight affects compressive strength and the development of C-S-H and N-A-S-H gels, which enhances mortar's mechanical

qualities [10]. High strength and a more stable microstructure are produced by a well-proportioned mix of alkali solution with NP. Najimi and Ghafoori have also demonstrated similar results for the usage of SS and SH with WGP in mortar [11].

Although alkali-activated cementitious composites can achieve a greater level of sustainability through cement replacement, the materials are often brittle and exhibit a low tensile capacity. Alex et al. (2024) studied the application of a combination of PPF (0.05–0.20% of the weight of the cement) and Diatomite Earth (DE) (5–20% of the cement) as partial cement replacements in concrete [12]. The outcome of their test indicated that the mixing of PPF produced a slight reduction in workability but with the addition of DE, a significant improvement in flexural, split tensile and compression strength was noted when matched with the control mix. The durability performance, including water penetration, chloride permeability and sorptivity resistance, of the best combination of 15% DE and 0.15% PPF was also improved, indicating the effectiveness of PPF in developing durable and mechanically robust sustainable concrete [12].

Although both natural pozzolan (NP) and WGP have been studied individually, there are fewer studies on the use of both as pozzolanic admixtures in alkali-activated mortars reinforced with polypropylene fibers (PPFs). Also, these materials have never been systematically evaluated with respect to their interaction with alkali activators and the impact of this interaction on the strength of the mortar. To systematically investigate the influences of NP, WGP, PPF and curing age on the compressive strength, flexural strength and split tensile strength of alkali-activated mortar, the optimal custom design (OCD) in RSM is applied. A total of 45 experimental mixes tested at 7, 28 and 90 days, as reported in our previous study [1], were used. RSM was also employed to develop prediction models, study interaction effects between the input factors, and determine optimum proportions of the mix. This statistical approach makes it possible to develop high-performance and sustainable alkali-activated mortars, as it provides a useful tool for understanding the interactions of several parameters through a limited number of tests. The novelty of the present study is the development of RSM prediction models, the evaluation of the interaction effects, and the optimization of the mix proportions. A summary of the previous studies on sustainable cementitious and optimization techniques is presented in Table 1.

Table 1. Summary of previous studies on sustainable cementitious materials incorporating waste glass powder and optimization techniques.

No.	Reference	Research Focus	Materials Used	Methodology	Key Findings	Research Gap
1	[13]	Alkali-activated slag mortar	Slag + waste glass powder	RSM (CCD), ANOVA	Optimum GP ≈14.6% and alkali content ≈8.3%; improved strength and sulfate resistance.	Only slag-based mortar considered; no fibers or AI-based prediction.
2	[8]	Pozzolanic behavior of WGP	Cement mortar + WGP	Experimental, SEM, XRD, FTIR, TGA	20% fine WGP enhanced later-age strength and microstructure.	No optimization model or statistical design; no alkali activation.
3	[14]	Prediction of flexural strength	Concrete with eggshell powder + WGP	ANN vs. RSM	ANN predicted flexural strength more accurately than RSM.	Limited to flexural strength; experimental validation was limited.

Table 1. *Cont.*

No.	Reference	Research Focus	Materials Used	Methodology	Key Findings	Research Gap
5	[15]	Reactive powder concrete optimization	Waste glass + micro $CaCO_3$	Multi-objective optimization	Reduced cement while maintaining high RPC performance.	Focused on RPC; did not investigate alkali-activated mortars.
6	[16]	Review and modeling of WGP mortar	Waste glass powder mortar	Review, MLR, ANN	ANN outperformed MLR in predicting compressive strength.	Review study; lacks new experimental optimization.
7	[17]	Sustainable concrete	Waste glass sand	RSM, microstructure	About 30% WGS improved strength and durability.	Studied aggregate replacement rather than binder replacement.
8	[18]	Fiber-reinforced concrete	Banana fiber + WGP	RSM	Optimum BF and GP improved compressive strength.	Considered only compressive strength; no geopolymer system.
10	[19]	One-part geopolymer mortar	GGBS, diatomite, feldspar	Experimental, SEM, XRD, FTIR	SNF improved workability and mechanical properties.	Focused on admixtures rather than waste glass optimization.
11	[20]	Fiber-reinforced geopolymer mortar	Coal waste + recycled glass + PPF	Experimental, SEM, FTIR, XRD	PPF improved flexural strength and optimized curing enhanced overall performance.	Did not use statistical optimization (RSM).
12	[21]	SCC prediction	Natural tuff + recycled glass	RSM, SVM, ANN	ANN showed the highest prediction accuracy; RSM remained effective.	Focused on self-compacting concrete rather than mortar.
13	[22]	Sustainable concrete optimization	Recycled glass powder + nano-silica	Taguchi optimization	15% RGP + 1% NS produced optimum mechanical and durability performance.	Used Taguchi instead of RSM; no alkali activation or fibers.

2. Materials

The experimental work in [1] aimed to elucidate the effect of replacing cement partially with NP and WGP in combination with alkali activation, using SS and SH, on the mechanical properties of mortar. PPF was also incorporated into the mixture to enhance the durability and reinforcement.

Qassim Cement meets ASTM C150 criteria because of its high strength, durability and its suitability for general purpose use [23]. The criteria for preparing mortar for this investigation are Type I. Local sand from the Qassim region with a specific gravity of 2.7 (ASTM C128) and fineness modulus of 2.6 (ASTM C136) was used for this study. This means that it is in the normal range for natural sands and thus has good density and mineral composition [24]. The Saudi NP used in this investigation was obtained from volcanic rocks in the west of KSA. It has a specific surface area of 667 m^2/kg and a specific gravity of 3.0.

All the glass waste was collected from windowpanes, glass doors and partition panels which were discarded during building construction. These materials were chosen due

to the sustainability of using a precious building resource made from non-biodegradable waste products. Discarded glass was gathered, cleaned to remove impurities, and then dried for preparation for grinding. The ground glass powder was obtained by grinding with a planetary ball mill. This was performed for 7 cycles at 400 rpm in order to achieve an effective reduction in particle size. A total of 10 kg of powdered glass was formed, with an average particle size of 75 μm.

SH and SS solutions were obtained from a local business in Saudi Arabia. SH is a strong alkaline activator which dissolves silica and alumina precursors and facilitates the geopolymerization process in NP and WGP. SS (or water glass) is a source of silicate and contributes to the mechanical strength and binding properties of the geopolymer matrix. Together, they create an alkaline environment, which is a requirement for the processes of dissolution and polycondensation used in geopolymer synthesis. The PPF used had the average length (12 mm) and diameter (18 microns) of microfilament fibers with specific gravity 0.91. Polypropylene fibers enhance the durability of cement mortar by increasing the tensile strength and reducing shrinkage, thus making it more resistant to cracking. The chemical composition of cement, NP, and WGP is shown in Table 2.

Table 2. XRF analysis of cement, NP, and WGP.

Components	Cement	NP	WGP
CaO	63.9	11.7	60.7
SiO_2	19.97	41.1	27.1
Al_2O_3	5.83	18.9	3.9
Fe_2O_3	3.43	0.09	2.5
MgO	0.61	3.62	2.3
SO_3	2.87	0.18	1.5
K_2O	0.71	1.1	0.45
Na_2O	0.159	0.31	0.91

3. Research Methodology

The experimental data used in the present study was obtained from our previously published study [1]; no new specimens were cast or tested for this study. The aim of the experimental research was to find the influence of cement replacement using NP and WGP on the mechanical characteristics of mortar. Another material used in the mixture was PPF, which was added to enhance the durability and reinforcement of the mixture. A flowchart of the methodology used in the research is shown in Figure 1.

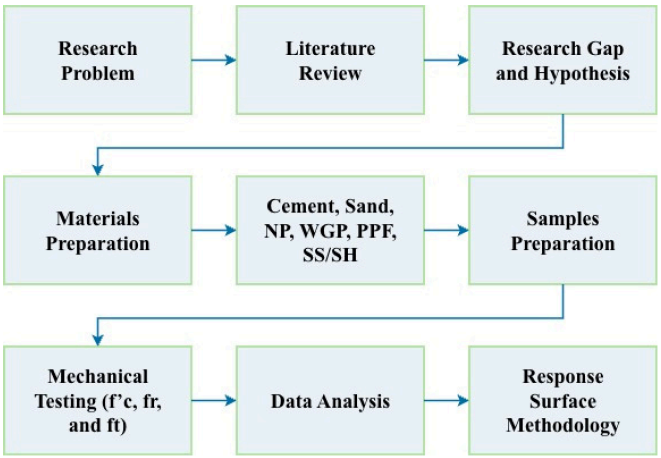


Figure 1. Research methodology.

The four input variables were NP, WGP, PPF, and Age (curing age), while the three outputs were fc, ft, and fr of mortar. Based on the data from the experimental work, regression models were selected. These parameters were chosen to give a detailed description of the factors that affect model predictions. Table 3 describes the levels of input parameters.

Table 3. Levels of the input parameters.

Parameter	Symbol	Unit	Level 1	Level 2	Level 3	Level 4
Natural pozzolan	NP	%	0	10	20	
Waste glass powder	WGP	%	0	10	20	30
polypropylene fibers	PPF	%	0	0.5	1.5	
Curing age	Age	day	7	28	90	

The dataset of [1] consists of 45 mixtures including 9 repeated mixtures as shown in Appendix A, and each mixture was tested at 7, 28 and 90 days for compressive, flexural and split tensile strength, which gives 135 runs and 405 test results. Separate specimens were cast for each curing age and each specimen was tested only once. Each test result is the average of three specimens, so the total number of specimens is 1215 (45 mixtures × 3 ages × 3 tests × 3 specimens). The cubes (50 mm × 50 mm × 50 mm) for CS, the prisms (40 mm × 40 mm × 160 mm) for flexural strength, and the cylindrical (100 mm diameter × 200 mm height) samples for split tensile strength were cast using the mortar proportions of ASTM C109, while the flexural and split tensile tests were carried out according to ASTM C348 and ASTM C496, respectively [25,26]. The samples were manufactured using cement and sand at a ratio of 1 to 2.75 and a water–cement ratio of 0.485 according to ASTM C109 requirements.

The process outlined in ASTM C 305 [27] was followed to create the mechanical mix. Before being added to the mortar, the alkaline solutions SH and SS were combined for ten minutes at room temperature. Batches of the necessary amounts of cement, sand, NP, WGP, and PPF were calibrated and combined. First, these ingredients were slowly combined by hand for three minutes. Then, using a slow-speed mixing device, during the wet mixing stage, the water and alkali solution was mixed for two minutes. This was followed by five minutes of mixing until a homogenous mixture was reached. A flow table was used to test the workability, as seen in Figure 2d, and superplasticizer was added to keep it at 110 mm± (Conplast SP430), sourced from Adwan Chemical Industry, Riyadh, Kingdom of Saudi Arabia. The molds were oiled lightly to demold and prevent sticking. For samples of cubes and prisms, the molds were filled in two layers and for cylinders a three-layered mold-filling technique was used, followed by 25 strokes of a tamping rod for each to remove the trapped air. The surface was smoothed by troweling the extra material. The specimens were delicately removed after 24 ± 2 h of casting, taking care not to damage them. Samples were placed in clear saturated lime water in a curing tank at 23 ± 2 °C immediately after demolding. All specimens were kept immersed until tested (7, 28 and 90 days). Cubic, prismatic, and cylindrical mortar samples were subjected to the compression testing machine after 7, 28 and 90 days of curing, following the ASTM C109, C348 and C496 standards respectively, to obtain the values of f'c, fr and ft.

3.1. Experimental Results

3.1.1. Compressive Strength (fc)

The compressive strength of alkali-activated mortar with different amounts of waste glass powder (WGP), polypropylene fibers (PPF), and natural pozzolan (NP) after 7, 28, and 90 days of standard curing is shown in Figure 3. All mixes showed an overall increase in compressive strength with curing age, which is indicative of the ongoing pro-

duction of alkali-activated reaction products and matrix densification. With a fiber dosage increase to 1.5%, the strength generally decreased, which may be due to the agglomeration of the fibers, the presence of a greater amount of trapped air, and reduced mortar workability, which resulted in a lower strength. Compressive strength of fiber contents was found to be highest when 0.5% PPF was included for all of them. The effects of precursor composition, on the other hand, indicated that a higher NP level (10%) generally led to higher compressive strength compared to higher WGP replacements.



(**a**) (**b**) (**c**) (**d**)

Figure 2. (**a**) Compressive strength test. (**b**) Flexural strength test. (**c**) Split tensile strength test. (**d**) Flow table test.

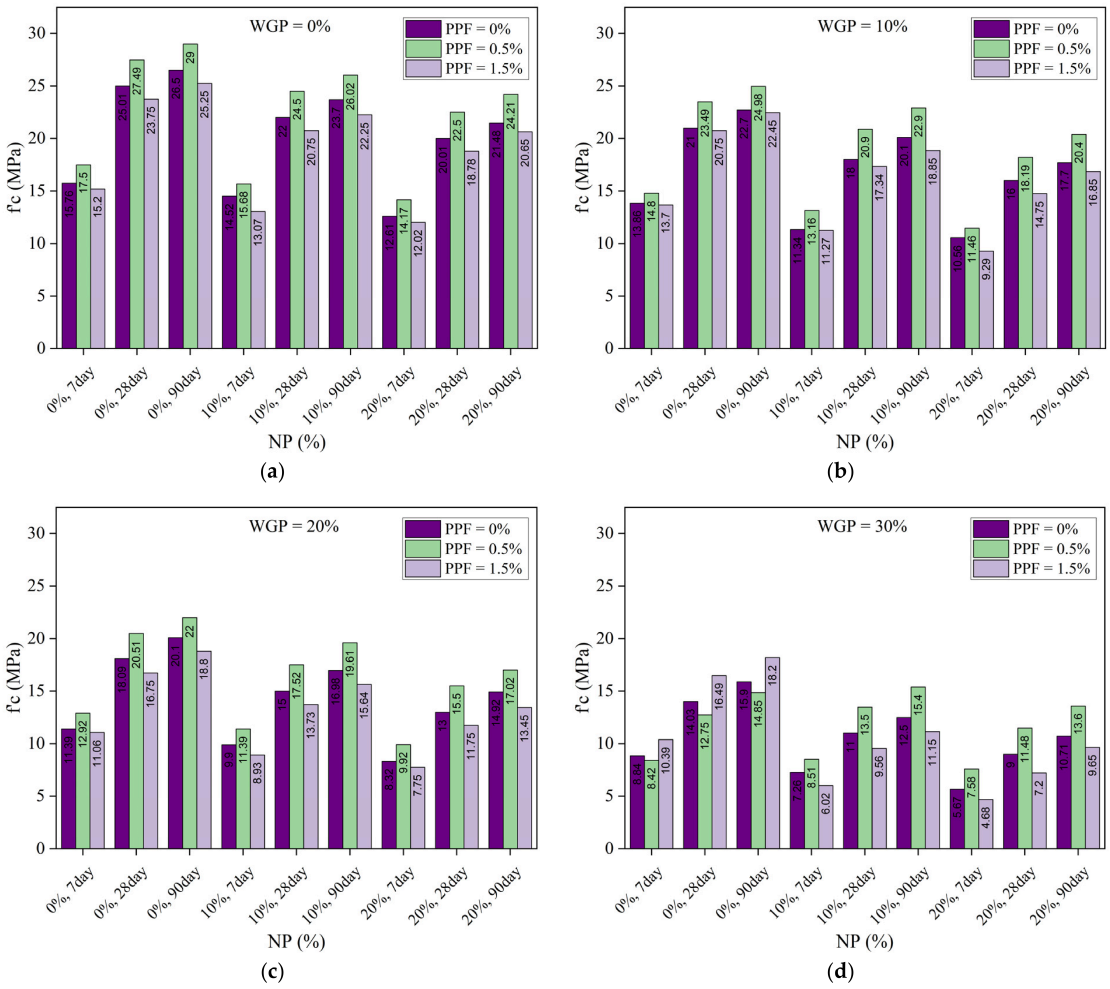


Figure 3. Effect of NP and PPF on fc: (**a**) 0% WGP; (**b**) 10% WGP; (**c**) 20% WGP; and (**d**) 30% WGP. Data from [1].

Approximately 29 MP of maximum compressive strength was obtained at 0% NP, 0% WGP and 0.5% PPF after 90 days, which showed that there is an optimum ratio of alkali activation to pozzolanic reactivity. Conversely, the addition of 20% and more (particularly 30%) WGP significantly reduced the compressive strength, suggesting that excess WGP lowered the amount of reactive calcium and slowed down geopolymerization. These findings reveal that, although the excess WGP replacement has a negative effect on strength growth, despite a long curing period, the mechanical properties of alkali-activated mortar can be enhanced through the incorporation of moderate contents of NP and WGP.

3.1.2. Splitting Tensile Strength (ft)

Alkali-activated mortar with different curing ages (7, 28, 90 days) is designed to use different proportions of NP, WGP and polypropylene fibers (PPF), with the results displayed in Figure 4. The beneficial crack bridging properties of the fibers in delaying the initiation and propagation of fractures under tensile loading were demonstrated by the addition of 0.5% PPF, which generally gave high ft, but the optimum content of PPF depended on the combined use NP and WGP. However, no further improvement was found when PPF was 1.5%, and in several mixes, it actually reduced the tensile strength due to agglomeration of fibers, and, due to lowering the workability, the porosity of the mix increased.

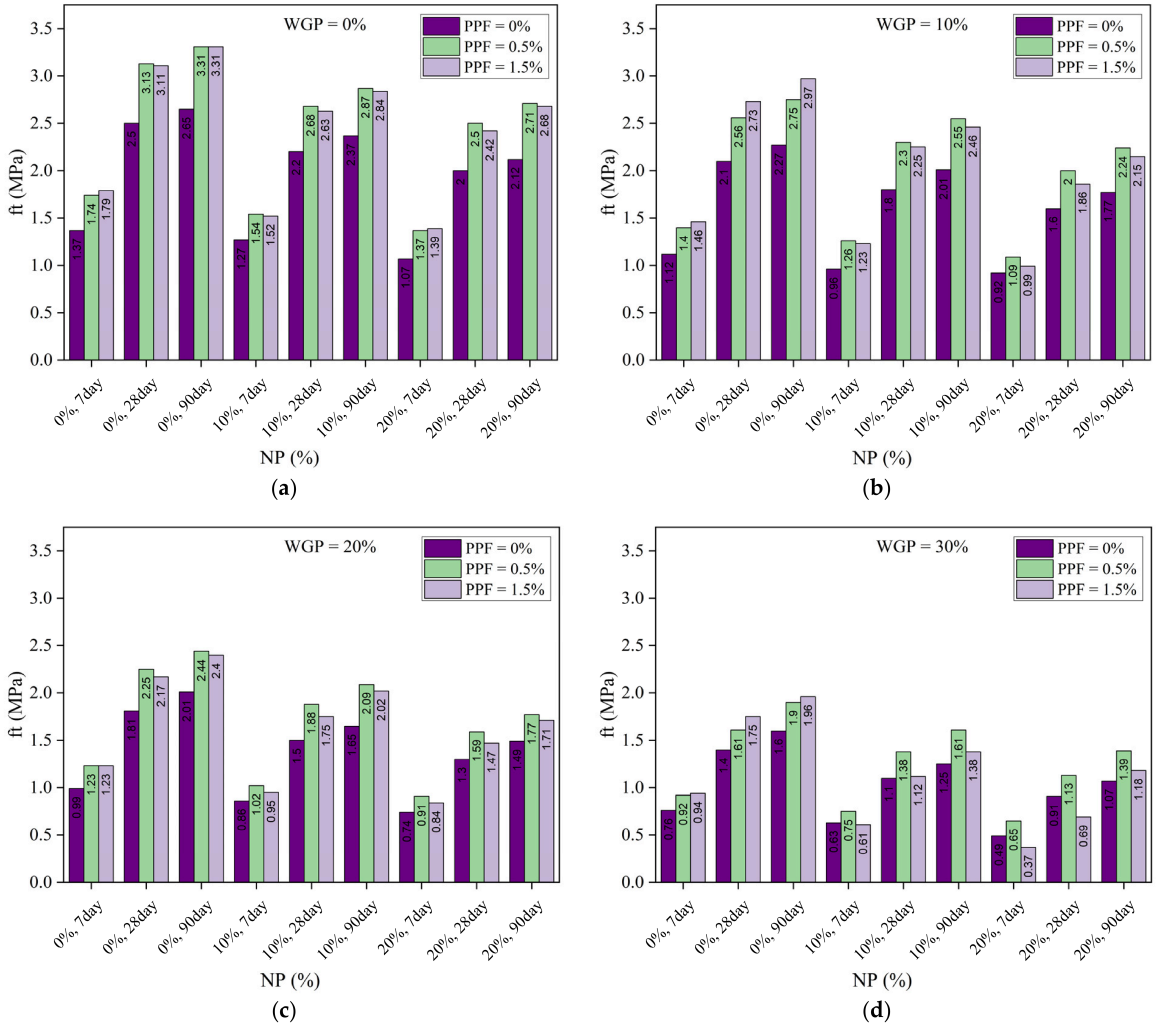


Figure 4. Effect of NP and PPF on ft: (**a**) 0% WGP; (**b**) 10% WGP; (**c**) 20% WGP; and (**d**) 30% WGP. Data from [1].

The best tensile strength was obtained for the precursor combination of mixtures containing 10% NP and 0 to 10% WGP (0.5% PPF) after 90 days with a tensile strength of approximately 3.3 MPa. This means that moderate pozzolan replacement and alkali activation have a synergistic effect. In contrast to the curing time, however, the tensile strength of the glass powder was seen to be decreasing with increasing concentration of WGP, especially at 30%, suggesting that too much glass powder hindered the formation of a dense reaction matrix. In summary, it could be concluded that excessive replacement of WGP has negative effects on the tensile performance of alkali-activated mortar, but moderate replacement of NP and WGP as well as an optimum fiber dosage of 0.5% PPF can significantly enhance the tensile performance of alkali-activated mortar.

3.1.3. Flexural Strength (fr)

For alkali-activated mortar, the fr varies according to the NP, WGP, PPF and curing time, as illustrated in Figure 5. Flexural strength started increasing from 7 days till 90 days, similar to compressive and split tensile strength. This indicates that geopolymerization is still in progress and that the binder matrix is denser and has been cured for longer. Adding 0.5% PPF always yielded the best flexural strength, which showed that polypropylene fibers can bridge microcracks and enhance the crack resistance and post-cracking properties under bending loads.

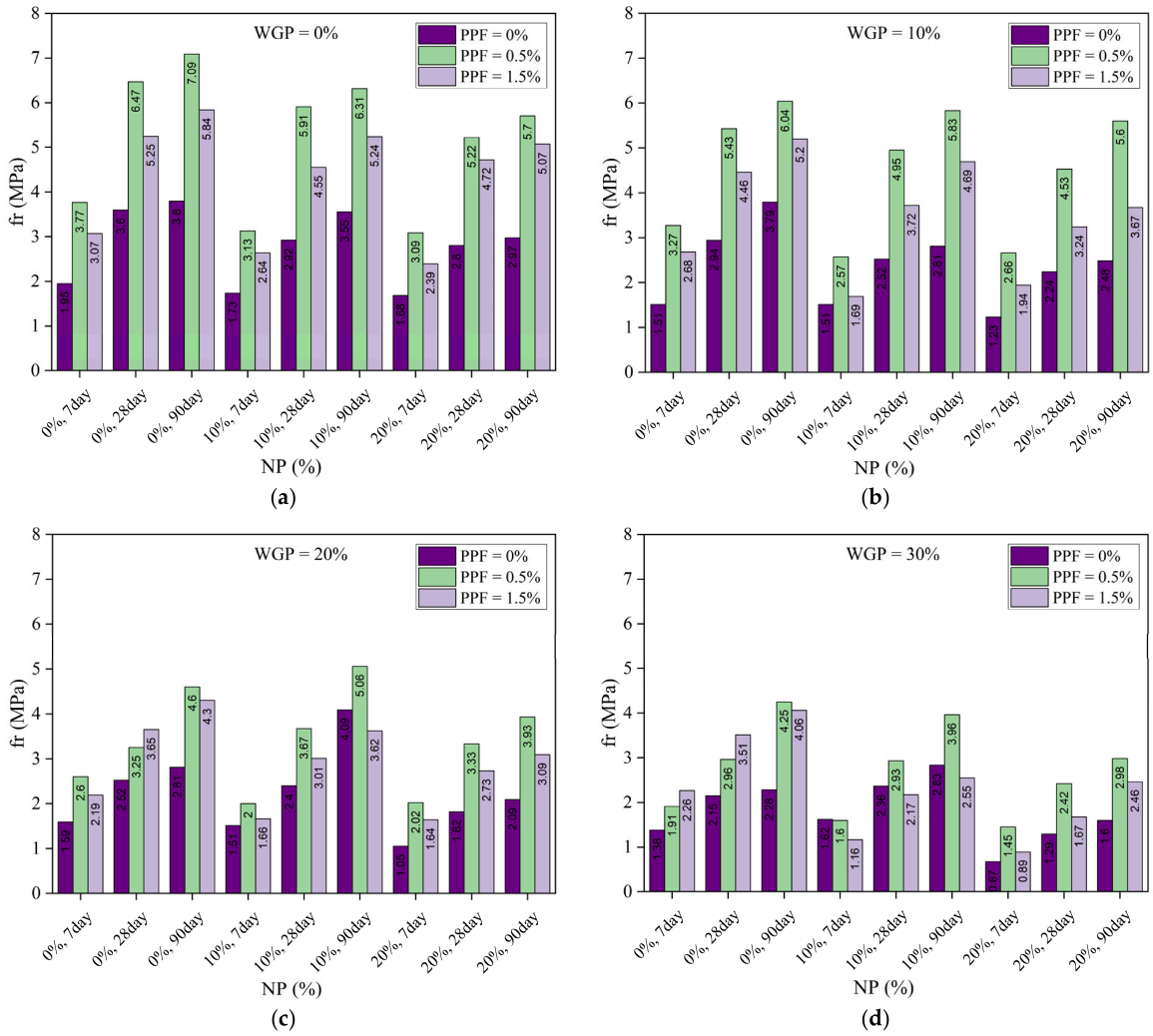


Figure 5. Effect of NP and PPF on fr: (**a**) 0% WGP; (**b**) 10% WGP; (**c**) 20% WGP; and (**d**) 30% WGP. Data from [1].

The flexural strength, however, tended to be slightly reduced as the concentration of fiber was increased to 1.5% PPF. The maximum fr of approximately 7.0 MPa was achieved for the mixtures that had 0% WGP, 0% NP and 0.5% PPF among the precursor combinations after 90 days. As the WGP replacement level increased to 20% and 30%, there was a noticeable reduction in fr for all curing ages, highlighting the negative effects of a high content of glass powder on the development of a thick alkali-activated matrix. The overall results indicate that the most favorable flexural results are obtained when using a low to moderate replacement level of both NP and WGP and an optimum fiber dose of 0.5% PPF.

4. Modeling and Methodology

4.1. Data Description

Response surface methodology (RSM) was conducted on the data, and the descriptive statistics for the experiment are presented in Table 4. NP, WGP, PPF and curing age were independent. NP ranged from 0 to 20%, WGP from 0 to 30%, PPF from 0 to 1.5%, and curing age from 7 to 90 days. The response variables were f'c, fr and ft. Their respective ranges were 4.68 to 29.02 MPa, 0.67 to 7.09 MPa, and 0.37 to 3.31 MPa. The mean values of f'c, fr and ft were found to be 16.24 MPa, 3.21 MPa and 1.75 MPa, respectively, with standard deviations of 5.51, 1.43 and 0.70 MPa, respectively, which showed that the experimental responses were sufficiently diverse to construct trustworthy models. All variables were found to have a skewness value between 0.044 and 0.563, which was considered to be approximately symmetrical with little positive skewness. Furthermore, the all-negative kurtosis values (−1.526 to −0.451) showed that all of the distributions were platykurtic, which is comparatively flatter than the normal distribution. Considering all the statistical properties, it can be concluded that the dataset is adequately spread and the distribution of the input and output variables is balanced, thus favoring the development and validation of trustworthy RSM models.

Table 4. Descriptive statistics of the data.

Variable	Unit	Minimum	Maximum	Average	Standard Deviation	Skewness	Kurtosis
NP	%	0.00	20.00	8.8889	7.98007	0.203	−1.400
WGP	%	0.00	30.00	14.2222	10.89068	0.044	−1.293
PPF	%	0.00	1.50	0.6556	0.63324	0.400	−1.526
Age	day	7.00	90.00	41.6667	35.36695	0.529	−1.511
f'c	MPa	4.68	29.02	16.2417	5.50765	0.205	−0.671
fr	MPa	0.67	7.09	3.2071	1.42775	0.563	−0.451
ft	MPa	0.37	3.31	1.7549	0.70144	0.308	−0.670

4.2. Correlation Coefficients

Amongst the input factors, the Pearson correlation heatmap in Figure 6 indicated that the curing age had a somewhat favorable correlation with the split tensile strength (r = 0.56), flexural strength (r = 0.53) and compressive strength (r = 0.53) of mortar, indicating that the strength of mortar continued to increase with time. Conversely, the mechanical properties had a smaller negative correlation with NP, and WGP content had the highest negative correlation with the compressive strength (r = −0.64). Split tensile strength and flexural strength were very weakly positively associated with PPF (r = 0.17 and 0.22, respectively). Mechanical parameters showed good correlation, especially between f'c and ft (r = 0.95), where an increase in one parameter was accompanied by an increase in the other.

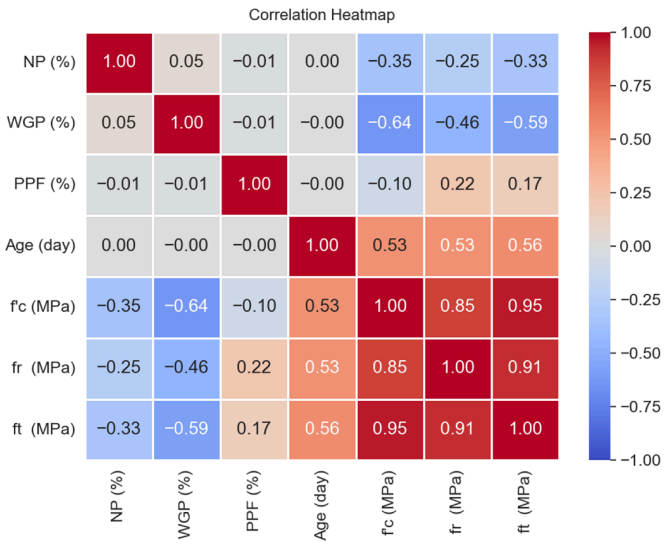


Figure 6. Pearson correlation coefficient heatmap.

The distribution and pairwise relationships of the input variables and mechanical qualities are shown in Figure 7. Strong positive linear relationships exist between f'c, fr, and ft, as illustrated by scatter plots, while diagonal plots illustrate the distribution of the experimental data. The input variables (NP, WGP, PPF and curing time), on the other hand, do not seem to have a continuous distribution, but rather a discrete one corresponding to the experimental levels chosen, and appear to be non-multicollinear. The overall shape of the pairplot indicates that experimental data is eligible for RSM modeling because there are no signs of inconsistencies and there is a general increase in one mechanical feature when the other increases.

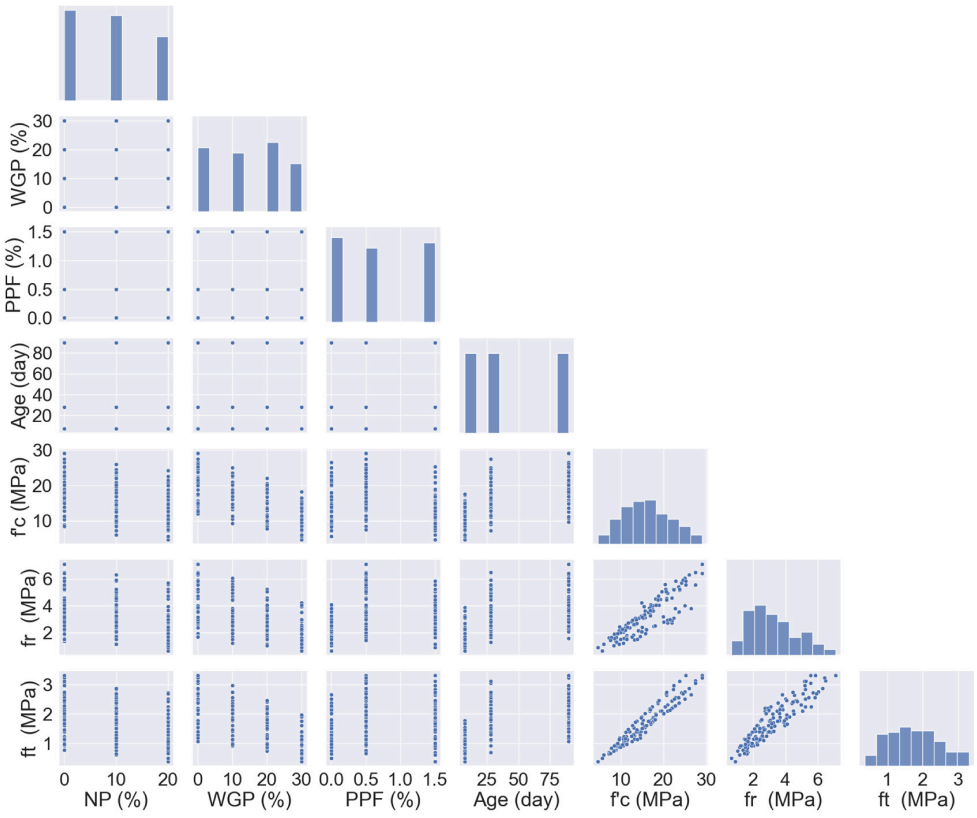


Figure 7. Pairwise plots.

4.3. Response Surface Methodology (RSM)

RSM is a statistical and mathematical optimization method which is used to find the interaction among many independent factors and response variables. In this work, RSM was used to analyze the effects of the variables (NP, WGP, PPF, and curing age) on f'c, fr and ft. The advantage of RSM is that it is able to provide predictive regression models estimate the effects of variable interactions and establish optimal proportion mixing with fewer experimental trials. The first-order (linear) regression model is expressed by Equation (1), while the second-order (quadratic) polynomial model, which accounts for linear, quadratic, and interaction effects, is given by Equation (2). The quadratic model is generally preferred in material optimization because it provides a more accurate representation of the nonlinear behavior of cementitious composites.

$$Y = \omega_o + \omega_1 X_1 + \omega_2 X_2 + \cdots \omega_k X_k + error \quad (1)$$

$$Y = \omega_o + \sum_{i=1}^{k} \omega_i X_i + \sum_{i=1}^{k} \omega_{ii} X_j^2 + \sum_{i<} \sum_{j} \omega_{ij} X_i X_j + error \quad (2)$$

4.4. Statistical Analysis and Model Selection

ANOVA results shown in Table 5 confirm that quadratic RSM models for f'c, fr, and ft are statistically significant ($p < 0.0001$). For all three responses, the main factors—NP (A), WGP (B), PPF (C), and curing age (D)—had significant effects on the mechanical properties. WGP and curing age exhibited the highest F-values, indicating that they were the most influential variables governing strength development. Several interaction terms were also significant, including AD and BD for compressive strength; BC, BD, and CD for flexural strength; and AC, AD, BC, BD, and CD for split tensile strength, demonstrating the combined influence of the input variables. In addition, significant quadratic terms (A^2, C^2, and D^2) confirmed the nonlinear behavior of the responses. The lack of fit was significant for the three models ($p < 0.05$). This is mainly because the pure error is very small (the replicate results were very close to each other), so even small systematic deviations become significant. The high R^2, adjusted R^2 and predicted R^2 values and the diagnostic plots show that the models are still adequate for prediction and optimization within the studied range.

Table 5. Summary of ANOVAs.

Response	Source	Sum of Squares	df	Mean Square	F-Value	*p*-Value	
fc	Model	3997.51	9	444.17	825.32	<0.0001	significant
	A-NP	425.43	1	425.43	790.5	<0.0001	
	B-WGP	1583.29	1	1583.29	2941.96	<0.0001	
	C-PPF	25.06	1	25.06	46.57	<0.0001	
	D-AGE	1421.14	1	1421.14	2640.66	<0.0001	
	AD	6.41	1	6.41	11.9	0.0008	
	BD	23.63	1	23.63	43.91	<0.0001	
	A^2	4.15	1	4.15	7.7	0.0064	
	C^2	176.21	1	176.21	327.42	<0.0001	
	D^2	520.46	1	520.46	967.08	<0.0001	
	Residual	67.27	125	0.5382			
	Lack of Fit	66.19	98	0.6754	16.89	<0.0001	significant
	Pure Error	1.08	27	0.0400			
	Cor Total	4064.78	134				

Table 5. *Cont.*

Response	Source	Sum of Squares	df	Mean Square	F-Value	*p*-Value	
fr	Model	251.58	9	27.95	161.94	<0.0001	significant
	A-NP	15.67	1	15.67	90.79	<0.0001	
	B-WGP	56.96	1	56.96	329.96	<0.0001	
	C-PPF	22.03	1	22.03	127.64	<0.0001	
	D-AGE	96.1	1	96.1	556.71	<0.0001	
	BC	2.41	1	2.41	13.94	0.0003	
	BD	1.18	1	1.18	6.82	0.0101	
	CD	0.7333	1	0.7333	4.25	0.0414	
	C^2	59.18	1	59.18	342.82	<0.0001	
	D^2	25.9	1	25.9	150.01	<0.0001	
	Residual	21.58	125	0.1726			
	Lack of Fit	19.49	98	0.1989	2.57	0.0033	significant
	Pure Error	2.09	27	0.0774			
	Cor Total	273.15	134				
ft	Model	64.45	12	5.37	441.32	<0.0001	significant
	A-NP	6.12	1	6.12	503.23	<0.0001	
	B-WGP	22.1	1	22.1	1815.69	<0.0001	
	C-PPF	1.88	1	1.88	154.08	<0.0001	
	D-AGE	25.6	1	25.6	2103.82	<0.0001	
	AC	0.1855	1	0.1855	15.24	0.0002	
	AD	0.1553	1	0.1553	12.76	0.0005	
	BC	0.4027	1	0.4027	33.09	<0.0001	
	BD	0.4624	1	0.4624	38	<0.0001	
	CD	0.1491	1	0.1491	12.25	0.0007	
	A^2	0.0861	1	0.0861	7.07	0.0089	
	C^2	2.06	1	2.06	169.42	<0.0001	
	D^2	10.18	1	10.18	836.52	<0.0001	
	Residual	1.48	122	0.0122			
	Lack of Fit	1.43	95	0.01505	8.00	<0.0001	significant
	Pure Error	0.0508	27	0.00188			
	Cor Total	65.93	134				

The most important terms in the generated models of RSM are listed in Table 6. The main effects of NP, WGP, PPF and curing age were significant for each response. WGP × Age and NP × Age had the most significant interaction term on compressive strength (f'c); WGP × PPF, WGP × Age, and PPF × Age had a significant interaction term on flexural strength (fr); the most significant interaction terms for ft were under 10%. In addition to this, the quadratic terms, NP^2, PPF^2 and Age^2, are significant, further proving the nonlinear behavior of the mechanical properties and therefore the application of quadratic RSM models for prediction and optimization.

Table 7 presents the fit statistics of RSM models. All exhibited high coefficients of determination (R^2 = 0.9210–0.9835), indicating excellent consensus among the predicted and actual results, as the adjusted R^2 and predicted R^2 values confirm the robustness and predictive capability of models without overfitting. Low coefficients of variation (C.V. = 4.52–12.95%) demonstrate good experimental precision and reliability, while the high Adeq Precision values (54.40–127.58), which are well above the recommended value

of 4, indicate an adequate signal and confirm that the models are suitable for navigating the design space and optimizing the mechanical properties of alkali-activated mortar.

Table 6. Important terms of model for all outcomes.

Model	Important Terms
f'c	NP, WGP, PPF, AGE, NP × AGE, WGP × AGE, NP^2, PPF^2, AGE^2
fr	NP, WGP, PPF, AGE, WGP × PPF, WGP × AGE, PPF × AGE, PPF^2, AGE^2
ft	NP, WGP, PPF, AGE, NP × PPF, NP × AGE, WGP × PPF, WGP × AGE, PPF × AGE, NP^2, PPF^2, AGE^2

Table 7. Fit statistics of all the outcomes.

Model	Standard. Deviation	Mean	CV %	R^2	Adjusted R^2	Predicted R^2	Adequate Precision
fc	0.7336	16.24	4.52	0.9835	0.9823	0.9807	127.5803
fr	0.4155	3.21	12.95	0.921	0.9153	0.9077	54.3968
ft	0.1103	1.75	6.29	0.9775	0.9753	0.9722	92.9321

The proposed quadratic regression models for f'c (Equation (3)), fr (Equation (4)), and ft (Equation (5)) describe the relationships between the input variables (NP, WGP, PPF, and curing age) and the corresponding mechanical properties of alkali-activated mortar. The models incorporate significant linear, interaction, and quadratic terms identified through ANOVA, enabling accurate prediction of the responses within the experimental range. The inclusion of quadratic and interaction terms captures the nonlinear behavior of variables and their combined effects on strength development. Owing to their high predictive accuracy and statistical significance, these equations can be effectively used to estimate and optimize the mechanical performance of alkali-activated mortar.

$$f'_c = 13.928 - 0.265NP - 0.269WGP + 6.818PPF + 0.444AGE - 0.00078NP \times AGE - 0.0011WGP \times AGE + 0.0037NP^2 - 5.008PPF^2 - 0.0033AGE^2 \quad (3)$$

$$f_r = 1.459 - 0.04295NP - 0.035WGP + 5.151PPF + 0.0984AGE - 0.019699WGP \times PPF - 0.000244WGP \times AGE + 0.00332PPF \times AGE - 2.902PPF^2 - 0.00074AGE^2 \quad (4)$$

$$f_t = 1.051 - 0.0269NP - 0.0249WGP + 1.131PPF + 0.0606AGE - 0.0074NP \times PPF - 0.00012NP \times AGE - 0.0081WGP \times PPF - 0.00015WGP \times AGE + 0.0015PPF \times AGE + 0.00053NP^2 - 0.5417PPF^2 - 0.00047AGE^2 \quad (5)$$

4.5. Diagnostic Plots

The compressive strength (f'c) model diagnostic plots are presented in Figure 8. The externally studentized residuals are randomly distributed around zero and stay within the control limits (±3.66) in the residuals versus run plot (Figure 8a), demonstrating the lack of outliers and systematic errors. The plot of predicted versus actual compressive strength (Figure 8b) reveals excellent agreement between experimental and predicted compressive strengths with predicted values roughly aligned with the 45° reference line. The results indicate that the quadratic RSM model developed can be adopted to successfully predict the compressive strength of alkali-activated mortar and it is statistically valid and reliable.

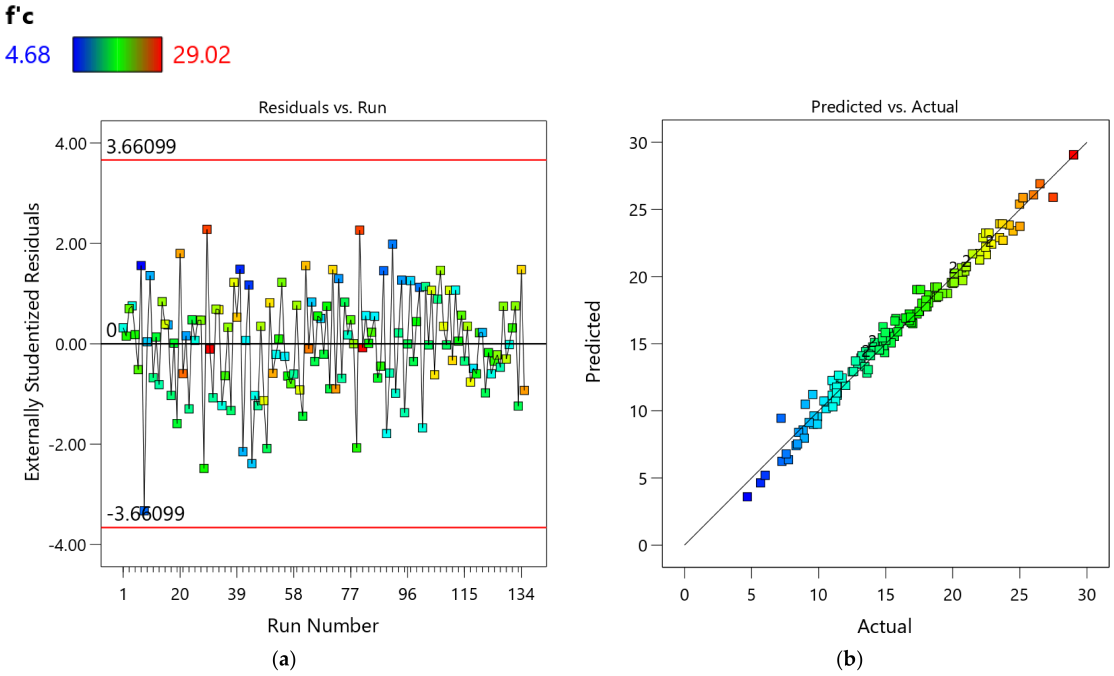


Figure 8. Diagnostic plots for the fc model: (**a**) studentized residuals vs. runs plots; (**b**) predicted responses vs. experimental values (MPa).

The split tensile strength (ft) model's diagnostic charts are shown in Figure 9. The externally studentized residuals are randomly distributed around zero and fall within the control limits (±3.66) in the residuals vs. run plot (Figure 9a), suggesting that there are no outliers or systematic trends. The data points near the 45° reference line in the plot of expected vs. actual values (Figure 9b) indicate a good alignment between the predicted and experimental values. The results confirmed that the developed quadratic RSM model is suitable, accurate and reliable for predicting the split tensile strength of alkali-activated mortar.

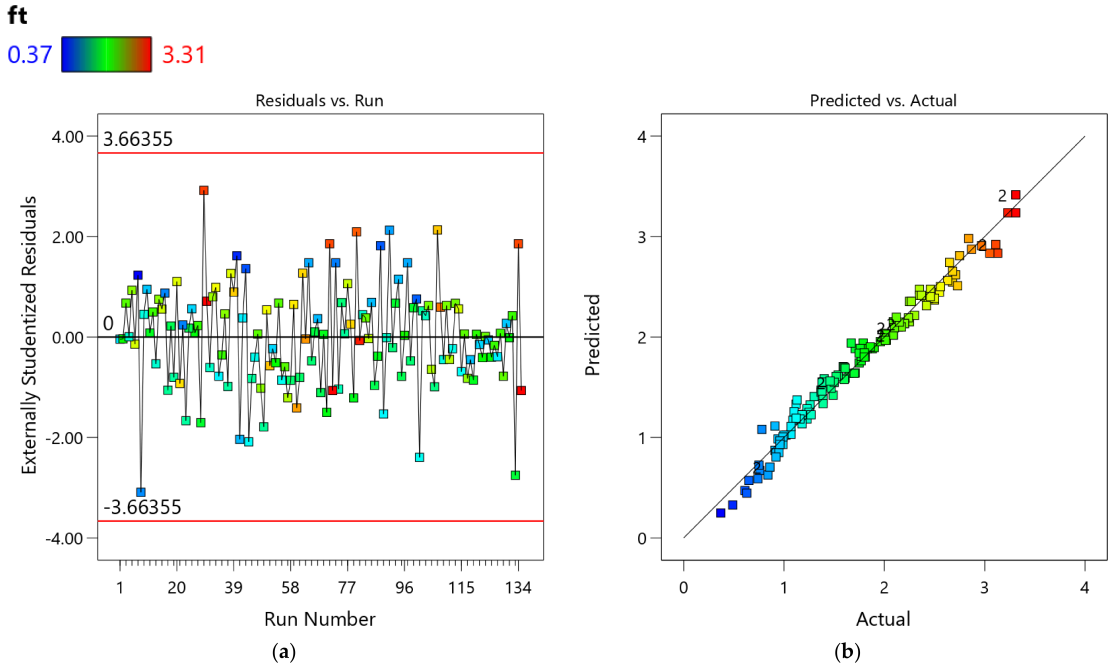


Figure 9. Diagnostic plots for ft model: (**a**) studentized residuals vs. runs plots; (**b**) predicted responses vs. experimental values (MPa).

The flexural strength (fr) model's diagnostic charts are shown in Figure 10. The flexural strength obtained from the experimental outcomes are aligned with the predicted results as shown in the expected versus actual plot (Figure 10b), which shows that the values predicted are closer to the 45° reference line. The absence of outliers and systematic errors is further confirmed by the plot of the studentized residuals against the runs (Figure 10a) where the externally studentized residuals are exhibiting a random distribution around zero and are not exceeding the control limits of ±3.66. These findings show that the quadratic RSM model that was created is statistically sufficient, dependable, and able to forecast the flexural strength of alkali-activated mortar with accuracy.

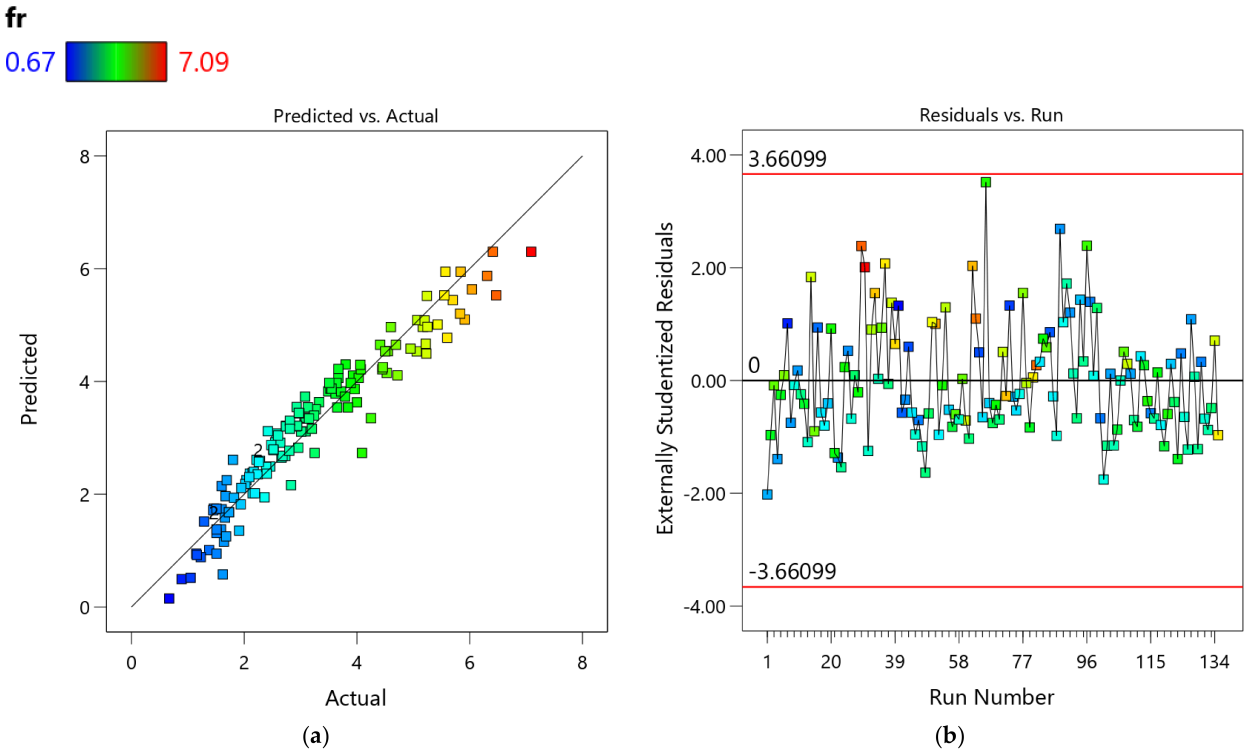


Figure 10. Diagnostic plots for the fr model: (**a**) studentized residuals vs. runs plots; (**b**) predicted responses vs. experimental values (MPa).

4.6. Synergistic Effect Plots

The combined effects of the input variables on the mechanical properties are shown by the 2D and 3D response surface plots in Figures 11–13. For all three strengths, the curing age had the largest positive effect, and increasing WGP content reduced the strength at all ages. The curved surfaces along the PPF axis confirm the significant PPF^2 term, where strength increased up to a moderate fiber content and then decreased at 1.5% PPF. The interaction plots of NP and WGP with curing age show that the reduction in strength by replacement did not disappear at later ages.

4.7. Optimization Results

The response surface methodology (RSM) desirability function was utilized to examine the mixture combinations that had the highest expected response within the experimental design space. In this optimization study, NP, WGP and PPF were regarded as mixture components while curing age was used as an experimental element. The optimization was carried out in the ranges of the studied variables, and the obtained solutions were evaluated based on the predicted response and the related desirability value.

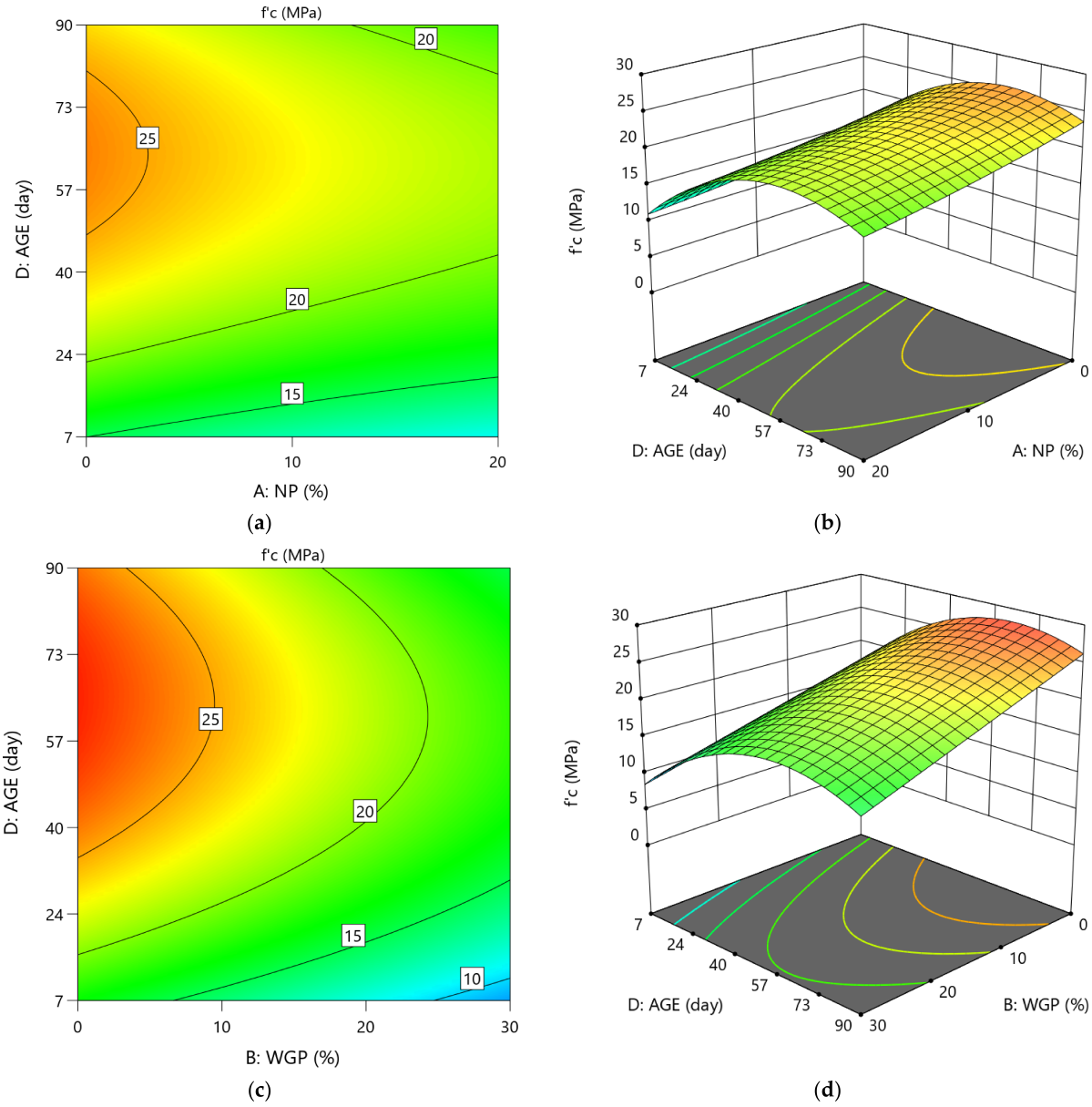


Figure 11. Response surface plots showing the effect of (**a**) natural pozzolan (NP) content and curing age, (**b**) their combined interaction in the three-dimensional response surface, (**c**,**d**) waste glass powder (WGP) content and curing age on the compressive strength f′c of the developed mortar.

The optimization results are shown in Table 8. The optimal mixture of the 28-day compressive strength contained 19.786% NP, 9.313% WGP and 0.969% PPF with a predicted compressive strength of 18.628 MPa and desirability value of 0.529. The optimization for the 90-day compressive strength gave a mixture of 14.554% NP, 9.031% WGP and 1.009% PPF with a predicted compressive strength of 21.281 MPa and desirability value of 0.568.

Table 8. Maximizing compressive strength (fc) with maximum NP and WGP.

AGE (Day)	NP (%)	WGP (%)	PPF (%)	f′c (MPa)	Desirability
28	19.786	9.313	0.969	18.628	0.529
90	14.554	9.031	1.009	21.281	0.568

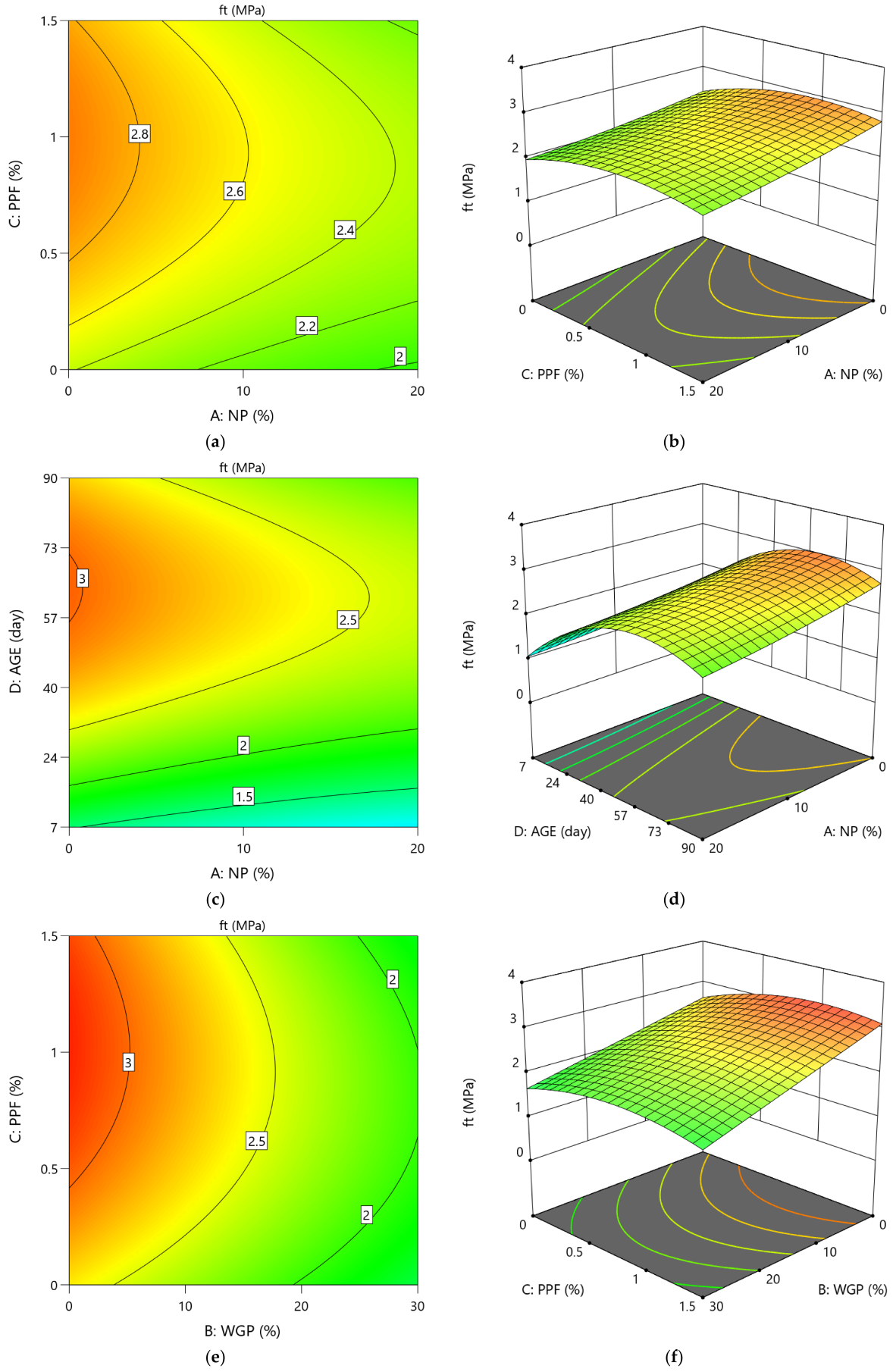


Figure 12. *Cont.*

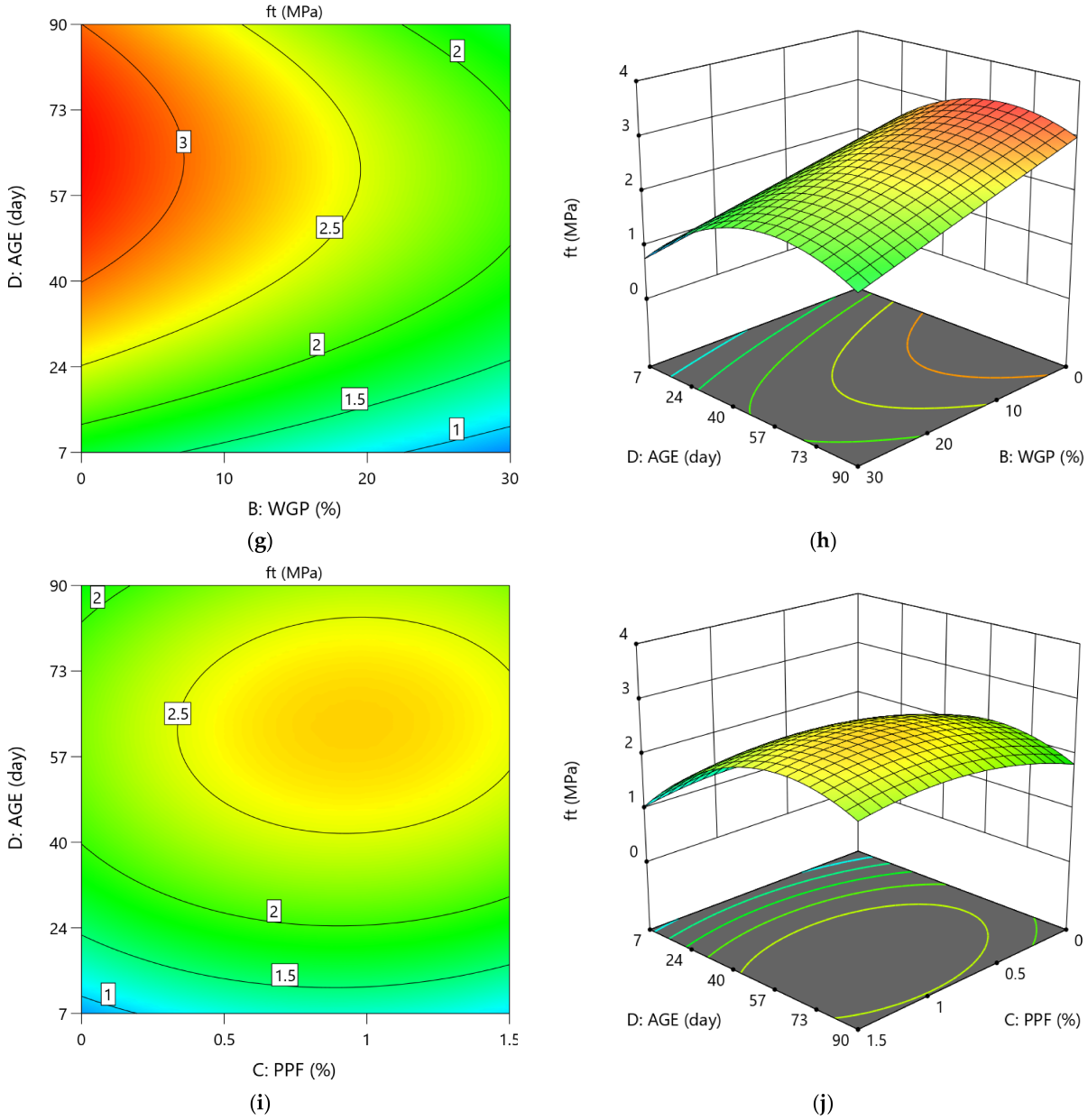


Figure 12. Contour and three-dimensional response surface plots illustrating the interactive effects of (**a**,**b**) NP and PPF contents, (**c**,**d**) NP content and curing age, (**e**,**f**) WGP and PPF contents, (**g**,**h**) WGP content and curing age, and (**i**,**j**) PPF content and curing age on the split tensile strength ft of the developed mortar.

Optimization results for the maximum split tensile strength are displayed in Table 9 and were obtained using the desirability function. Based on the optimized solution, the optimal content should be approximately 9% WGP, 13–20% NP and 1.2–1.3% PPF and the maximum expected tensile strength can be found. The 90-day solution (NP = 12.708%, WGP = 8.731%, PPF = 1.319%) also got highest expected ft of 2.517 MPa and its desirability value of 0.60 was the best. Based on these results, the tensile strength of the alkali-activated mortar can be increased by increasing curing time, NP content and WGP content, and slightly reducing the PPF content.

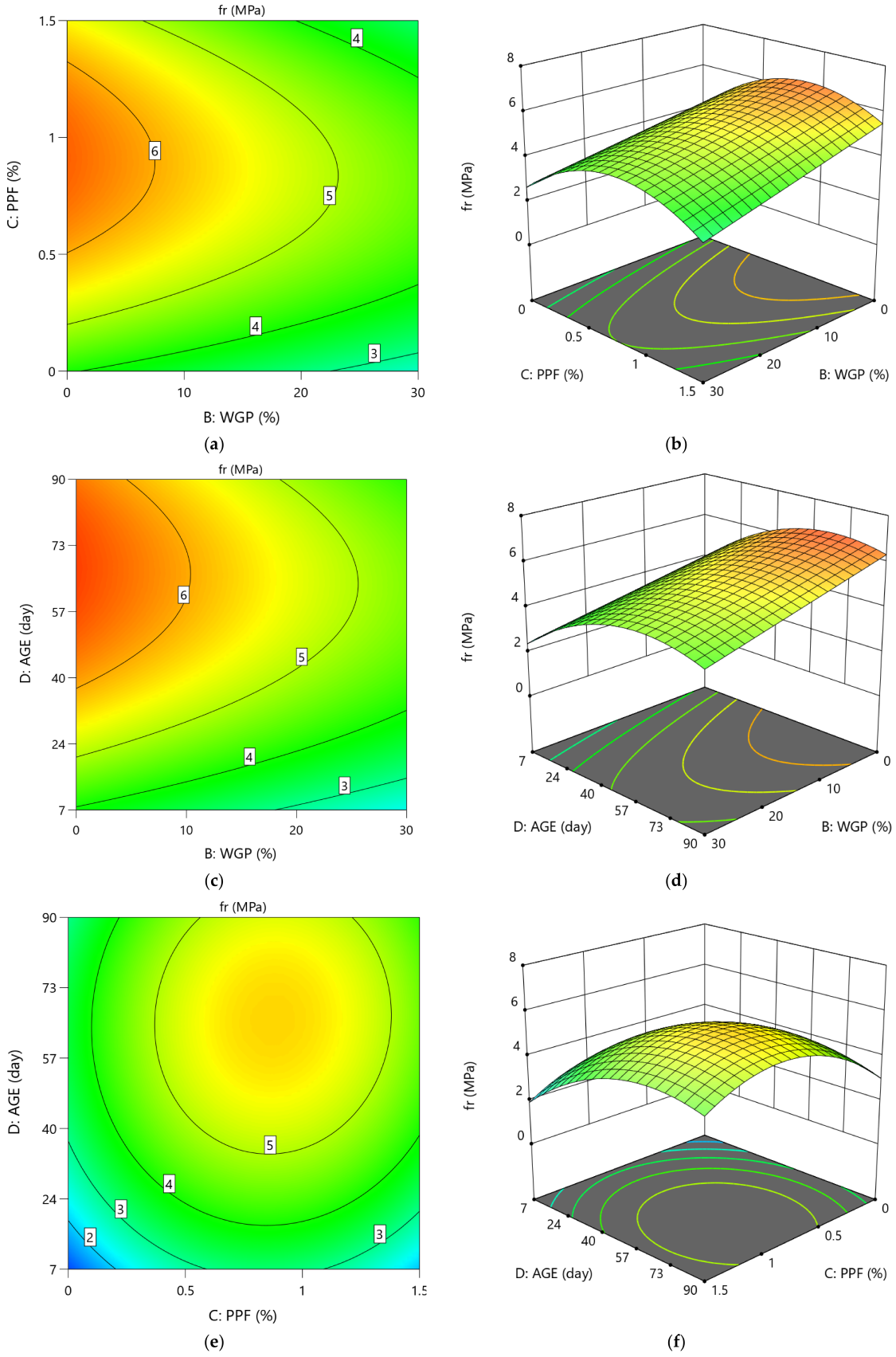


Figure 13. Contour and three-dimensional response surface plots showing the effects of (**a**) WGP and PPF contents, (**b**) WGP and PPF contents, (**c**) WGP content and curing age, (**d**) WGP content and curing age, (**e**) PPF content and curing age, and (**f**) PPF content and curing age on the flexural strength fr of the developed mortar.

Table 9. Maximizing tensile strength (ft) with maximum NP and WGP.

AGE (Day)	NP (%)	WGP (%)	PPF (%)	f't (MPa)	Desirability
28	19.999	9.046	1.159	2.106	0.55
90	12.708	8.731	1.319	2.517	0.6

The optimization results for maximizing flexural strength obtained with the desirability function are presented in Table 10. The best solution reveals that the maximum flexural strength is obtained with approximately 11–12% WGP, 18–20% NP, and approximately 1.0% PPF. The solution with the highest desirability of 0.615 and the highest expected flexural strength of 5.086 MPa among the optimized solutions was the 90-day solution (NP = 20%, WGP = 11.373%, PPF = 1.045%). The results indicate that the flexural properties of alkali-activated mortars are improved by higher curing time, medium WGP content and the optimum dosage of PPF.

Table 10. Maximizing flexural strength (fr) with maximum NP and WGP.

AGE (Day)	NP (%)	WGP (%)	PPF (%)	f'r (MPa)	Desirability
28	17.661	12.35	0.993	4.46	0.552
90	20	11.373	1.045	5.086	0.615

The results of multi-response optimization (concurrently optimizing split tensile, flexural and compressive strengths) are presented in Table 11. The optimum solutions indicate that about 5% NP, 4% WGP, and 1.0% PPF will yield the best overall mechanical performance. With an overall desirability of 0.704 and the greatest anticipated f'c (25.489 MPa), fr (6.299 MPa), and ft (3.039 MPa), the 90-day optimized mix (NP = 5.46%, WGP = 4.097%, PPF = 1.004%) outperformed the 28-day solution. The result of these findings indicates that the best balance of all three mechanical qualities has been obtained with longer curing time, lower NP and WGP replacement rates and the optimum PPF replacement rate.

Table 11. Maximizing fc, ft, and fr with maximum NP and WGP.

AGE (Day)	NP (%)	WGP (%)	PPF (%)	f'c (MPa)	f'r (MPa)	f't (MPa)	Desirability
28	5.537	4.438	0.957	22.878	5.485	2.655	0.624
90	5.46	4.097	1.004	25.489	6.299	3.039	0.704

5. Conclusions

- The generated quadratic RSM models showed good coefficient of determination values (R2 = 0.921 to 0.984) and the diagnostic plots showed that the models can be used for prediction within the studied range of compressive, flexural and split tensile strength for mortar samples.
- Based on the ANOVA results, all mechanical attributes were greatly affected by NP, WGP, PPF and curing age, with curing age and WGP being the most significant variables affecting the strength of mortar.
- Mechanical properties became better as the curing age increased and alkali-activated mortar showed better performances when moderate replacement rates of NP and WGP were used with ideal content of PPF. Too much WGP substitution negatively affected strength.

- Multi-objective optimization revealed that the optimum mix of 5.46% NP, 4.10% WGP, and 1.00% PPF with 90 days of curing had the best mechanical output of 25.49 MPa (compressive), 6.30 MPa (flexural), and 3.04 MPa (split tensile).

Author Contributions: Conceptualization, M.I.K., M.K.A. and H.A.D.; methodology, M.I.K., M.K.A. and H.A.D.; software, H.A.D. and M.I.K.; validation, M.K.A.; formal analysis, H.A.D.; investigation, M.I.K., M.K.A. and H.A.D.; resources, M.K.A.; experimental work, M.I.K. and M.I.; writing—original draft preparation, M.I.K.; writing—review and editing, H.A.D. and M.K.A.; visualization, M.I.K. and M.I.; supervision, M.K.A. and H.A.D.; project administration, M.K.A. and M.I.; funding acquisition, M.K.A. All authors have read and agreed to the published version of the manuscript.

Funding: This research received no external funding.

Data Availability Statement: All the raw data supporting the conclusion of this paper were provided by the authors.

Acknowledgments: The Researchers would like to thank the Deanship of Graduate Studies and Scientific Research at Qassim University (https://www.qu.edu.sa (accessed on 4 October 2026)) for financial support (QU-APC-2026).

Conflicts of Interest: The authors declare no conflicts of interest.

Abbreviation

NP	Natural Pozzolan
WGP	Waste Glass Powder
SCMs	Supplementary Cementitious Materials
SH + SS	Sodium Hydroxide + Sodium Silicate
PPF	Polypropylene Fiber
OPC	Ordinary Portland Cement
Age	Curing Age
f'c	Compressive Strength
fr	Flexural Strength
ft	Tensile Strength (or Split Tensile Strength)
R	Pearson's Correlation Coefficient
R^2	Coefficient of Determination
MPa	Megapascal
CO_2	Carbon Dioxide
RSM	Response Surface Methodology
ANOVA	Analysis of Variance
SCC	Self-Compacting Concrete
OCD	Optimal Custom Design
C.V.	Coefficients of Variation

Appendix A

Table A1. Mix design.

Mix	NP (%)	WGP (%)	PPF (%)
1	0	0	0
2	0	0	0.5
3	0	0	1.5
4	0	0	0.5
5	0	0	1.5

Table A1. *Cont.*

Mix	NP (%)	WGP (%)	PPF (%)
6	0	10	0
7	0	10	0.5
8	10	0	1.5
9	10	0	0.5
10	10	0	0
11	0	10	1.5
12	10	0	0
13	0	10	0
14	10	10	1.5
15	0	20	0.5
16	0	20	0
17	10	10	0.5
18	20	0	0.5
19	10	10	1.5
20	20	0	1.5
21	0	20	1.5
22	0	20	1.5
23	10	10	0
24	20	0	0
25	0	20	0
26	10	20	0.5
27	10	20	1.5
28	0	30	0
29	20	10	0.5
30	10	20	0.5
31	10	20	0
32	20	10	0
33	0	30	1.5
34	10	20	0
35	0	30	0.5
36	20	10	1.5
37	10	30	0.5
38	10	30	1.5
39	20	20	0.5
40	20	20	0
41	10	30	0
42	20	20	1.5
43	20	30	1.5
44	20	30	0
45	20	30	0.5

References

1. Khan, M.I.; Alkharisi, M.K.; Dahish, H.A. Performance of Sustainable Alkali-Activated Mortar Incorporating Natural Pozzolan, Waste Glass Powder, and Polypropylene Fibers. *Sustainability* **2026**, *18*, 53. [CrossRef]
2. Miller, S.A.; John, V.M.; Pacca, S.A.; Horvath, A. Carbon Dioxide Reduction Potential in the Global Cement Industry by 2050. *Cem. Concr. Res.* **2018**, *114*, 115–124. [CrossRef]
3. Guo, Y.; Luo, L.; Liu, T.; Hao, L.; Li, Y.; Liu, P.; Zhu, T. A Review of Low-Carbon Technologies and Projects for the Global Cement Industry. *J. Environ. Sci.* **2024**, *136*, 682–697. [CrossRef]
4. Ahmed, A. Assessing the Effects of Supplementary Cementitious Materials on Concrete Properties: A Review. *Discov. Civ. Eng.* **2024**, *1*, 145. [CrossRef]
5. Sharbaf, M.; Najimi, M.; Ghafoori, N. A Comparative Study of Natural Pozzolan and Fly Ash: Investigation on Abrasion Resistance and Transport Properties of Self-Consolidating Concrete. *Constr. Build. Mater.* **2022**, *346*, 128330. [CrossRef]
6. Khan, M.I.; Alhozaimy, A.M. Properties of Natural Pozzolan and Its Potential Utilization in Environmental Friendly Concrete. *Can. J. Civ. Eng.* **2011**, *38*, 71–78. [CrossRef]

7. Najimi, M.; Ghafoori, N.; Radke, B.; Sierra, K.; Sharbaf, M. Comparative Study of Alkali-Activated Natural Pozzolan and Fly Ash Mortars. *J. Mater. Civ. Eng.* **2018**, *30*, 04018115. [CrossRef]
8. Li, Q.; Qiao, H.; Li, A.; Li, G. Performance of Waste Glass Powder as a Pozzolanic Material in Blended Cement Mortar. *Constr. Build. Mater.* **2022**, *324*, 126531. [CrossRef]
9. Jochem, L.F.; Casagrande, C.A.; Onghero, L.; Venâncio, C.; Gleize, P.J.P. Effect of Partial Replacement of the Cement by Glass Waste on Cementitious Pastes. *Constr. Build. Mater.* **2021**, *273*, 121704. [CrossRef]
10. Adewumi, A.A.; Ismail, M.; Ariffin, M.A.M.; Yusuf, M.O.; Salami, H.O.; Owolabi, T.O.; Maslehuddin, M. Empirical Modelling of the Compressive Strength of an Alkaline Activated Natural Pozzolan and Limestone Powder Mortar. *Ceram. Silik.* **2020**, *64*, 407–417. [CrossRef]
11. Najimi, M.; Ghafoori, N. Engineering Properties of Natural Pozzolan/Slag Based Alkali-Activated Concrete. *Constr. Build. Mater.* **2019**, *208*, 46–62. [CrossRef]
12. Alex, A.G.; Jose, P.A.; Antony, M.R.; Dhanalakshmi, K. The Effect of Partial Replacement of Cement with Diatomaceous Earth (DE) and Polypropylene Fibers (PPF) on Fresh, Hardened, and Durability Properties of Concrete. *Int. J. Concr. Struct. Mater.* **2024**, *18*, 24. [CrossRef]
13. Zhang, L.; Yue, Y. Influence of Waste Glass Powder Usage on the Properties of Alkali-Activated Slag Mortars Based on Response Surface Methodology. *Constr. Build. Mater.* **2018**, *181*, 527–534. [CrossRef]
14. Liu, X.; AlAteah, A.H.; Alsubeai, A.; Alahmari, T.S.; Mostafa, S.A. Prediction of Flexural Strength of Concrete with Eggshell and Glass Powders: Advanced Cutting-Edge Approach for Sustainable Materials. *Rev. Adv. Mater. Sci.* **2024**, *63*, 20240055. [CrossRef]
15. Abellán-García, J.; Daza, N.; Molinares, M.; Abbas, Y.M.; Khan, M.I. Multi-Criteria Optimization of Cost-Effective and Environmentally Friendly Reactive Powder Concrete Incorporating Waste Glass and Micro Calcium Carbonate. *Materials* **2023**, *16*, 6434. [CrossRef]
16. Ahmad, S.A.; Ahmed, H.U.; Rafiq, S.K.; Mahmood, K.O.F.; Rostam, K.J.; Jafer, F.S. A Comprehensive Exploration on the Effect of Waste Glass Powder as a Partial Replacement of Cement in Mortar: A Review, Analysis, and Modeling Investigation. *Arab. J. Sci. Eng.* **2024**, *49*, 5721–5748. [CrossRef]
17. Baikerikar, A.V.; Navalgatti, N.; Ram, V.V.; Doshi, T.D. Modelling and Optimization of Waste Glass Sand in the Production of Sustainable Concrete Using Response Surface Methodology. *Iran. J. Sci. Technol. Trans. Civ. Eng.* **2025**, *50*, 4165–4188. [CrossRef]
18. Olukayode, O.M.; Akinwande, A.A.; Balogun, O.A.; Oyediran, A.O.; Mosuru, S.G.; Abdulwahid, M.Y.; Romanovski, V. Applicability of the Response Surface Method in the Optimization of Compressive Strengths of Banana-Fiber-Reinforced Concrete Using Waste Glass as Partial Cement Replacement. *Innov. Infrastruct. Solut.* **2023**, *8*, 207. [CrossRef]
19. Poojalakshmi, E.S.; Nagarajan, P.; Sudhakumar, J.; Thomas, B.S.; Das, S.; Berhe, M.A. Performance Evaluation of Superplasticizers in One Part Geopolymer Mortar. *Sci. Rep.* **2026**, *16*, 10892. [CrossRef]
20. Najafitabar, F.; Pourabbas Bilondi, M.; Ghaffarian, V. Polypropylene Fiber-Reinforced Geopolymer Mortar from Coal Washing Waste and Recycled Glass Powder: Mechanical and Microstructural Performance. *Sci. Rep.* **2026**, *16*, 21050. [CrossRef]
21. Bouzidi, M.A.; Bouziane, A.; Bouzidi, N. RSM, SVM and ANN Modeling of the Properties of Self-Compacting Concrete with Natural Mordenite-Rich Tuff and Recycled Glass. *Asian J. Civ. Eng.* **2025**, *26*, 89–106. [CrossRef]
22. Ul Haq, M.Z.; Singh, S.; Vora, T.; Ak, D.; Tomar, A.; Vanitha, S.; Das, P.; Thirugnanasambandam, A.; Kumar, V.V. Sustainable Concrete Mix Optimization with Recycled Glass Powder and Nano-Silica: A Taguchi Method Analysis. *J. Struct. Integr. Maint.* **2026**, *11*, 2546210. [CrossRef]
23. Specification for Portland Cement. Available online: https://store.astm.org/c0150_c0150m-24.html (accessed on 1 October 2025).
24. Test Method for Relative Density (Specific Gravity) and Absorption of Fine Aggregate. Available online: https://store.astm.org/c0128-12.html (accessed on 1 October 2025).
25. *ASTM C348*; Standard Test Method for Flexural Strength of Hydraulic-Cement Mortars. ASTM International: West Conshohocken, PA, USA, 1954.
26. Test Method for Splitting Tensile Strength of Cylindrical Concrete Specimens. 2017. Available online: https://store.astm.org/c0496_c0496m-17.html (accessed on 1 October 2025).
27. Practice for Mechanical Mixing of Hydraulic Cement Pastes and Mortars of Plastic Consistency. Available online: https://store.astm.org/c0305-20.html (accessed on 1 October 2025).

Disclaimer/Publisher's Note: The statements, opinions and data contained in all publications are solely those of the individual author(s) and contributor(s) and not of MDPI and/or the editor(s). MDPI and/or the editor(s) disclaim responsibility for any injury to people or property resulting from any ideas, methods, instructions or products referred to in the content.